DOI: 10.6060/ivkkt.20226507.6629

УДК: 537.528+541.15

ПЛАЗМЕННО-РАСТВОРНЫЙ СИНТЕЗ ОКСИДА ЦИНКА, ДОПИРОВАННОГО КАДМИЕМ

К.В. Смирнова, Д.А. Шутов, А.Н. Иванов, А.С. Манукян, В.В. Рыбкин

Кристина Валерьевна Смирнова (ORCID 0000-0001-8360-2346), Дмитрий Александрович Шутов (ORCID 0000-0002-4662-4631), Александр Николаевич Иванов (ORCID 0000-0002-5207-7582), Анна Славиковна Манукян, Владимир Владимирович Рыбкин (ORCID 0000-0001-7295-7803)*

Кафедра технологии приборов и материалов электронной техники, Ивановский государственный химико-технологический университет, Шереметевский просп., 7, Иваново, Российская Федерация, 153000
E-mail: rybkin@isuct.ru*

В данной работе исследован процесс образования нерастворимых соединений цинка и кадмия, инициированный действием разряда постоянного тока атмосферного давления в воздухе на водный раствор нитратов цинка и кадмия. Установлено, что, когда раствор является анодом, действие разряда приводит к образованию коллоидного раствора гидроксинитратов и гидроксидов цинка и кадмия белого цвета. Коллоидные частицы первоначально образуются на границе раздела раствор-разряд. И далее область образования распространяется в глубину раствора. С ростом времени действия разряда коллоидный раствор теряет свою агрегативную устойчивость и на дне реакционного сосуда начинает образовываться осадок. Кинетику образования коллоидных частиц исследовали турбидиметрическим методом. Оказалось, что скорость образования коллоидных частиц возрастает с увеличением разрядного тока от 30 до 70 мА. При концентрациях нитратов цинка и кадмия 50 ммоль/л константа скорости процесса увеличивается с $1{,}3\cdot10^{-3}$ до $12\cdot10^{-3}$ $с^{-1}$. При разрушении этого раствора образуется осадок соответствующих соединений. Рентгеноструктурный анализ показал, что частицы осадка имеют кристаллическую структуру. Частицы осадка, как показывает сканирующая электронная спектроскопия, имеют сфероидальную форму с характерным размером около 1 мкм. Термическое разложение образовавшегося осадка протекает в несколько стадий и заканчивается при температуре ~300 °С. В результате прокаливания образуется смесь кристаллических оксидов цинка и кадмия. По данным электронной рентгеновской спектроскопии, при мольном соотношении цинка и кадмия в исходном растворе 1:1 полученные твердые частицы содержат 8 мол. % кадмия и 92 % цинка.

Ключевые слова: газовый разряд, оксиды цинка и кадмия, коллоидный раствор, СЭМ, рентгено- и ТГА-анализ

PLASMA-SOLUTION SYNTHESIS OF ZINC OXIDE DOPED WITH CADMIUM

K.V. Smirnova, D.A. Shutov, A.N. Ivanov, A.S. Manukyan, V.V. Rybkin

Kristina V. Smirnova (ORCID 0000-0001-8360-2346), Dmitriy A. Shutov (ORCID 0000-0002-4662-4631), Aleksandr N. Ivanov (ORCID 0000-0002-5207-7582), Anna S. Manukyan, Vladimir V. Rybkin (ORCID 0000-0001-7295-7803)*

Department of Microelectronic Devices and Materials Technology, Ivanovo State University of Chemistry and Technology, Sheremetevskiy ave., 7, Ivanovo, 153000, Russia
E-mail: rybkin@isuct.ru*

In this work, the process of formation of insoluble zinc and cadmium compounds, initiated by the action of a direct current discharge of atmospheric pressure in air on an aqueous solution of zinc and cadmium nitrates, has been investigated. It was found that when the solution is the anode, the action of the discharge leads to the formation of a colloidal solution of zinc and cadmium hydroxynitrates and hydroxides of white color. The kinetics of the formation of colloidal particles was investigated by the turbidimetric method. It turned out that the rate of formation increases with an increase in the discharge current from 30 to 70 mA. At concentrations of zinc and cadmium

nitrates 50 mmol/l the rate constant of the process increases from $1.3 \cdot 10^{-3}$ to $12 \cdot 10^{-3}$ s^{-1}. When this solution is destroyed, a precipitate of the corresponding compounds is formed. X-ray analysis showed that the precipitate particles have a crystalline structure. The sediment particles, as shown by SEM, have a spheroidal shape with a characteristic size of about 1 μm. Thermal decomposition of the resulting precipitate proceeds in several stages and ends at a temperature of ~300 °C. As a result of calcination, a mixture of crystalline zinc and cadmium oxides is formed. According to EDX data, at a molar ratio of 1:1 of zinc and cadmium in the initial solution, the obtained solid particles contain 8 mol.% cadmium and 92% zinc.

Key words: gas discharge, zinc and cadmium oxides, colloidal solution, SEM, X-ray and TGA analysis

Для цитирования:
Смирнова К.В., Шутов Д.А., Иванов А.Н., Манукян А.С., Рыбкин В.В. Плазменно-растворный синтез оксида цинка, допированного кадмием. *Изв. вузов. Химия и хим. технология*. 2022. Т. 65. Вып. 7. С. 28–34. DOI: 10.6060/ivkkt.20226507.6629.

For citation:
Smirnova K.V., Shutov D.A., Ivanov A.N., Manukyan A.S., Rybkin V.V. Plasma-solution synthesis of zinc oxide doped with cadmium. *ChemChemTech* [*Izv. Vyssh. Uchebn. Zaved. Khim. Khim. Tekhnol*.]. 2022. V. 65. N 7. P. 28–34. DOI: 10.6060/ivkkt.20226507.6629.

INTRODUCTION

In recent years, semiconductor nanostructured materials have begun to be widely used due to their optical, electrical, and catalytic properties [1-3]. N-type semiconductors $A^{II}B^{VI}$ hexagonal ZnO and cubic cadmium oxide (CdO) were initially noted for their potential applications as transparent conducting oxides. ZnO is a promising candidate for light-emitting/detecting devices with high quantum efficiency, operating in the blue and ultraviolet (UV) regions, due to the straight wide band gap (3.37 eV) and high excitation binding energy (60 meV). CdO has a 2.5 eV direct band gap and an indirect band gap of 1.98 eV. Therefore, its use has promising prospects for the manufacture of solar cells, phototransistors, catalysts, and gas sensors. Taking into account the proximity of the radii of Zn and Cd and other basic properties, the inclusion of CdO in ZnO makes it possible to obtain ZnO / $Zn_{1-x}Cd_xO$ heterojunctions or superlattices, which are key elements in light emitting diodes based on ZnO. Doping with cadmium reduces the band gap and thereby changes the optical characteristics of the material, shifting the emission and absorption spectra into the visible region of the spectrum.

In the works known to us, the preparation of Cd-Zn-O by the sol-gel method [4], from solutions under high pressure [5], by the pyrolysis method [6], by chemical precipitation of hydroxides from solution [7], by filtered cathode arc deposition [8] has been investigated. A relatively new method for producing oxide materials is a method based on the action of a gas discharge on aqueous solutions of metal salts. This method, which is simpler from the above, was successfully applied for the synthesis of oxides of zinc, cadmium and iron (III) in works [9-11], respectively. The formation of insoluble zinc and cadmium compounds from aqueous solutions of their salts is also of interest from the point of view of water purification from heavy metal ions.

The aim of this work was to study the possibilities and features of the synthesis of mixed oxygen-containing compounds of zinc and cadmium under the action of a direct current discharge of atmospheric pressure in air on aqueous solutions of nitrates of these substances.

EXPERIMENTAL

In this work, we used aqueous solutions of zinc and cadmium nitrates (analytical grade) with a concentration of 50 mmol/l for each component. The experimental setup used in the study is described in detail by us in [10, 12]. Briefly, the discharge cell was H-shaped, consisting of two identical parts, 100 ml in volume, connected through a cellophane membrane. A direct current discharge was ignited above the solution surface in both cells in air at atmospheric pressure. Therefore, the solution in one part of the cell served as the anode (A-cell), and in the other, the cathode (C-cell). External electrodes were made of titanium. The electrode-solution distance was 5 mm. The discharge current could vary within 30-70 mA.

By the action of a discharge a colloidal solution was formed in the near-surface layer of A-cell and precipitate was formed at the bottom of the cell. The obtained sol-like fraction from top of the A-cell was collected by pipette, centrifuged and rinsed with distilled water. Washed sol was dried in ambient air at 60 °C for 24 h.

The kinetics of the colloidal particle formation process was investigated using the method of turbidimetry. The intensity of the light passing through the layer

(1 mm below the surface) of the solution was measured with an AvaSpec-2048 FT-2 spectrometer (Avantes, Netherlands). The optical length was 45 mm. The light source was a He-Ne laser (λ = 632.8 nm).

For qualitative and quantitative analysis of the phase composition of the powders, x-ray diffraction analysis was used (X-ray diffractometer DRON 3 M, Burevestnik, Russia, CuKα radiation). The diffraction patterns were processed using QualX2 software [13] and the open crystallographic COD database [14].

Thermogravimetric analysis (TGA) and differential scanning calorimetry (DSC) of the obtained precipitates were performed on a STA 449 F1 Jupiter thermal analysis instrument (Netzsch, Germany). The temperature range was 20 °C-900 °C at a heating rate of 5 °C min^{-1} in an argon flow using a platinum crucible.

The shape of the obtained particles, their sizes and elemental composition of the powder were obtained using scanning electron microscopy (SEM, Tesla Vega 3SBH, Czech Republic) with an EDX analysis system (Aztec EDS, Oxford Instruments Ltd., England).

RESULTS AND DISCUSSION

The action of the discharge leads to the formation of a colloidal solution in the liquid anode. Three minutes after ignition of the discharge, a white colloidal suspension was observed at the plasma-solution interface. As the plasma treatment proceeds, the particles grow larger and precipitate at the bottom of the cell. The formation of particles and sediment was not observed in the liquid cathode.

A typical form of the kinetic curve obtained by the turbidimetry is shown in Fig. 1. In the semi-logarithmic coordinates on the kinetic curve, two linear dependences are clearly observed. These data show that the process of formation of insoluble particles and their subsequent coagulation includes at least two stages. The presence of the first slow stage (induction period) indicates the threshold nature of the process. To start the coagulation process, a certain critical parameters of solution particles must be achieved.

The indicated sections of the kinetic curves are well described by an exponential function (determination coefficient $R^2 > 0.9$). Such processing allows one to determine effective rate constants or characteristic times. The results of such processing for the second (fast) section of the kinetic curve are shown in Fig. 2. Each point was obtained from five measurements.

An increase in the discharge current (Fig. 2) leads to an increase in the rate of formation of both colloidal particles and the rate of their coagulation. It is likely that an increase in the discharge current leads to an increase in the concentration of particles directly or indirectly involved in the formation of colloidal particles.

Unfortunately, data on the composition of active solution particles for both the liquid cathode and the liquid anode are very limited. Quantitative experimental data were obtained only for hydrogen peroxide. Thus, in studies [15, 16] for discharge current up to 40 mA, the concentration of hydrogen peroxide was several mmol/l in the liquid cathode. In a discharge with a liquid anode, the concentration of H_2O_2 at the same currents was an order of magnitude lower [17, 18]. An increase in the peroxide concentration was observed with an increase in the discharge current.

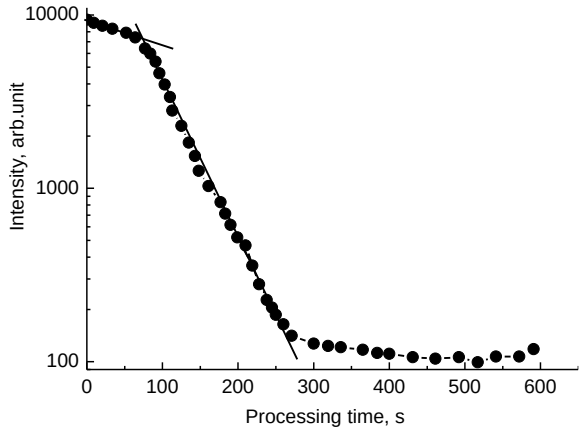

Fig. 1. The dependence of the normalized transmission of the solution on the processing time. Discharge current is 70 mA

Рис. 1. Нормированная зависимость пропускания раствора от времени обработки. Ток разряда 70 мА

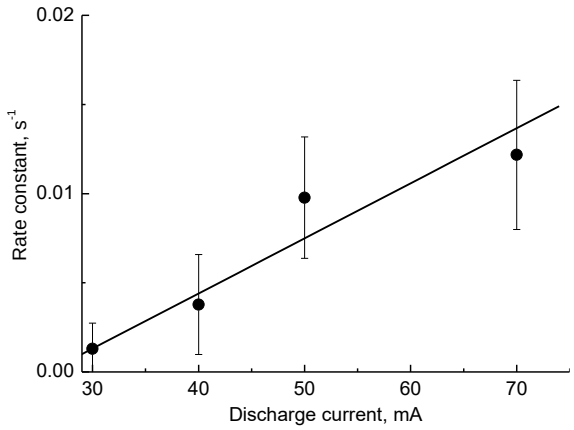

Fig. 2. The dependence of the effective rate constant on the discharge current

Рис. 2. Зависимость эффективной константы скорости от разрядного тока

We are not aware of the experimental results on measuring the concentrations of other active particles (OH, HO_2, H, etc.). The available data, which can apparently be used for estimates, are obtained as a result of numerical simulations. Simulation of the processes occurring during the action of the discharge on

water, which was the cathode of discharge, was carried out in [19]. A simulation of the processes initiated by the afterglow (absence of the action of charged particles) of a discharge in air was carried out in [20]. A similar simulation, but for a discharge with a liquid anode, was performed in [21]. In all cases, the qualitative composition of the formed particles was similar. An increase in concentrations was observed with an increase in the discharge current.

The possible reducing agents of the Cd^{2+} and Zn^{2+}in the solution are e_{solv} (solvated electrons), H and OH radicals and H_2O_2. The rate constants of reduction reactions, for example, Cd^{2+}+ H, Cd^{2+}+ OH, Cd^{2+}+ H_2O_2 are less than $5\cdot10^5$ l/(mol·s) [22]. The rate constant of reaction Cd^{2+}+ e_{solv} is equal to $5.4\cdot10^{10}$ l/(mol·s) [22]. The maximum concentrations of OH, H, H_2O_2 do not exceed 10^{-3} mol/l [15]. The concentration of solvated electrons reaches~ 1 mmol/l [23]. Consequently, solvated electrons should play a dominant role in the possible reduction of zinc and cadmium ions, since the corresponding reaction rate is five orders of magnitude higher than for other components.

Another important parameter of water is its pH. The impact of the discharge on the water cathode and the water anode leads to different results [24, 25]. The water in the cathode becomes acidic, and in the anode it becomes alkaline. For example, at a discharge current of 40 mA in an air atmosphere, the pH in the anode increases from 7 to 11, and in a liquid cathode, the pH decreases from 7 to 3 when the discharge operates for 300 s [24]. In the presence of an aqueous solution of a salt that is capable of hydrolysis, the quantitative picture of pH changes becomes different, but the qualitatively noted regularities remain [11]. In a liquid anode, the pH value is always higher than in a cathode. Apparently, the formation of an alkaline solution is associated with the following [23, 26]. The surface of the anode, unlike the cathode, is bombarded by a flux of electrons, which are rapidly solvated. As a result, their concentration in a surface layer with a thickness of the order of several nanometers reaches a value of about 1 mmol/l. The main reaction of the decay of solvated electrons is their reaction with water molecules, leading to the formation of hydroxide ions, that is, the formation of an alkaline medium.

$$H_2O + e_{solv} \rightarrow O + OH^- \quad (2K = 1.1\cdot10^{10}\ \text{l/(mol·s)}) \quad (1)$$

The rate of this reaction should increase with increasing discharge current. Since the concentration of water molecules is higher than the concentration of metal ions by three orders of magnitude, the solvated electrons are consumed by reaction (1), and not for the reduction of ions. At a high concentration of metal ions, they can probably be reduced to the metals themselves. For example, in [27], at a high concentration (the authors do not write how high) of silver nitrate, the formation of a colloidal solution of silver on the surface was observed. For this reason, it can be assumed that the resulting insoluble compounds are zinc and cadmium hyrodroxo compounds. Indeed, the products of solubility for equilibrium

$$Zn^{2+} + 2OH^- \leftrightarrow Zn(OH)_2\downarrow \quad (2)$$

$$Cd^{2+} + 2OH^- \leftrightarrow Cd(OH)_2\downarrow \quad (3)$$

are $2.2\cdot10^{-14}$ and $1.2\cdot10^{-17}$ for Cd and Zn, respectively. For a concentration of 50 mmol/l, the calculation gives the pH values at which precipitates of Zn and Cd hydroxides will be formed equal to 6.2 and 7.8, respectively. The deposition of zinc hydroxide is possible already in a weakly acidic environment, and cadmium hydroxide – in a weakly alkaline one. In addition, zinc hydroxo compounds are the first to precipitate, followed by cadmium. X-ray data support this conclusion.

The X-ray spectrum of the resulting powders is shown in Fig. 3.

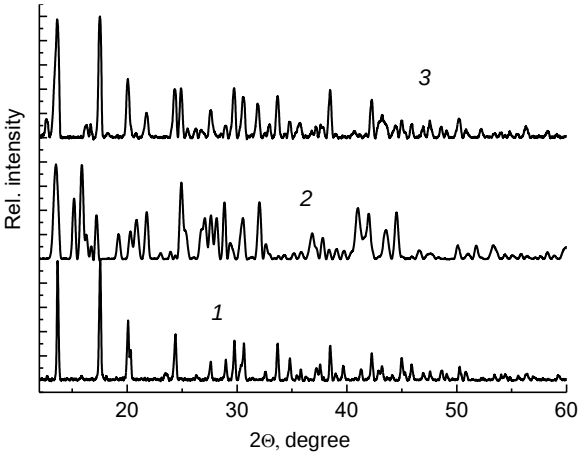

Fig. 3. XRD patterns for uncalcined synthesized powder. 1 - $Cd(NO_3)_2$ solution [10], 2 - $Zn(NO_3)_2$ solution [9]. 3 –$ZnCd(NO_3)_2$ solution
Рис. 3. Рентгенограммы непрокаленного синтезированного порошка. 1 – раствор $Cd(NO_3)_2$ [10], 2 – раствор $Zn(NO_3)_2$ [9], 3 – раствор $ZnCd(NO_3)_2$

The same figure shows the spectra of powders obtained under the same conditions from individual solutions of zinc nitrate and cadmium nitrate [9, 10]. Processing of spectra *1* and *2* showed that for cadmium they consist of crystalline phases $Cd(NO_3)OH\cdot H_2O$, β and γ $Cd(OH)_2$, and for zinc – from $Zn(NO_3)OH\cdot H_2O$ and $Zn(OH)_2$. It can be seen that the phase composition of powders obtained from solutions of a mixture of zinc and cadmium nitrates includes the same phases with a predominant content of phases including zinc compounds. Elemental analysis also showed that the powder contains zinc, cadmium, oxygen and nitrogen (Zn:Cd:N:O = 1:0.08:0.4:4.2).

The X-ray spectrum of the calcined powder is shown in Fig. 4. Spectra of calcined powders obtained separately from solutions of zinc nitrate (*2*) and cadmium nitrate (*1*) are also shown here. Spectra (*2*) and (*1*) correspond to zinc oxide (hexagonal structure) and cadmium oxide (cubic structure). It is seen that the spectrum of the powder obtained from solutions of a mixture of nitrates practically coincides with the spectrum of zinc oxide. At the same time, EDX analysis shows that the powder contains cadmium. The elemental composition of the powder corresponds to the $(CdO)_{0.08}$ x $(ZnO)_{0.92}$ formula. This discrepancy is due to the following. As already noted, due to the difference in solubility products, zinc hydroxo compounds are the first to precipitate, followed by cadmium. Therefore, the core of the resulting particles is represented by zinc compounds, while the shell of the particles is mainly represented by cadmium compounds. Due to the high penetrating ability of X-rays, X-ray analysis gives the average structure of the entire particle. EDX gives information about the state of the surface due to the low penetrating ability of electrons. The estimate of the penetration depth of electrons into the CdO using the Kanaya-Okayama formula gives a value of 0.15 μm for electron energy of 4 keV. Indeed, elemental EDX mapping shows that cadmium is located on the surface of sediment grains.

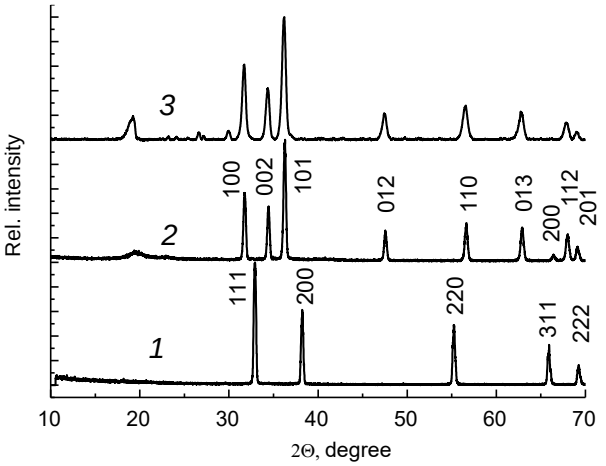

Fig. 4. XRD patterns for calcined synthesized powder. 1 - $Cd(NO_3)_2$ solution [10], 2 - $Zn(NO_3)_2$ solution [9]. 3 –$ZnCd(NO_3)_2$ solution
Рис. 4. Рентгенограммы прокаленного синтезированного порошка. 1 – раствор $Cd(NO_3)_2$ [10], 2 – раствор $Zn(NO_3)_2$ [9]. 3 – раствор $ZnCd(NO_3)_2$

SEM image of (ZnO-CdO) shows that the obtained powders are not homogeneous and contain a large number of pores. After high-temperature treatment, the particles acquire a spherical shape with a characteristic size of 1-2 μm (Fig. 5).

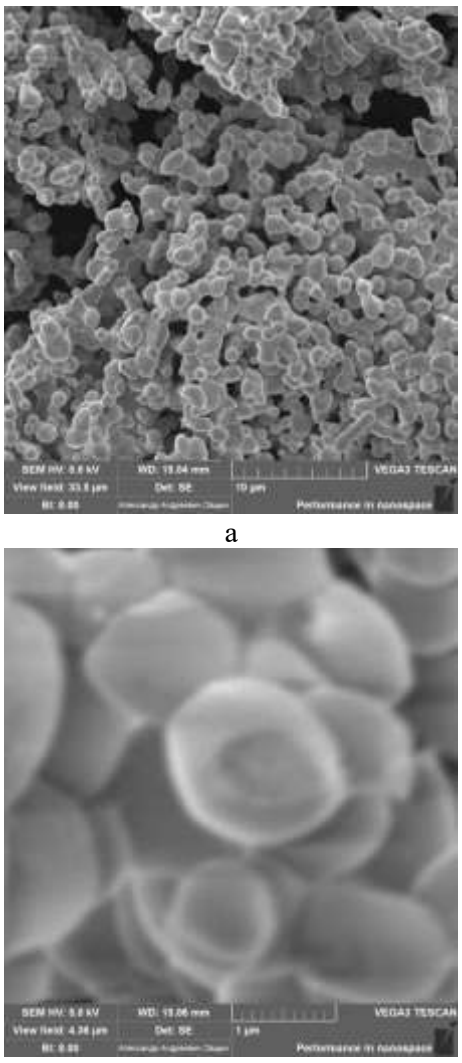

а

б

Fig. 5. SEM image of calcined synthesized powder
Рис. 5. СЭМ-изображение прокаленного синтезированного порошка

Fig. 6 shows the results of TGA analysis in the form of DSC curves. The same figure shows the results obtained in works [9, 10] for powders obtained by the action of a discharge on solutions of zinc nitrate and cadmium nitrate separately.

The presence of coinciding and non-coinciding extremes suggests that the compositions of the resulting powders are not just the sum of identical zinc and cadmium compounds. The absence of maxima in the range of 400-450 °C indicates the absence of cadmium nitrates and their formation during calcination, which decompose in this temperature range [10]. The extremum in the region of ~135 °C, which is common for a mixture of nitrates and zinc nitrate, indicates the decomposition of zinc hydroxide by the reaction $Zn(OH)_2 \rightarrow ZnO + H_2O$. The extremes coinciding for a mixture of nitrates and cadmium nitrate at ~215 °C

correspond to the decomposition of cadmium hydroxide according to the reaction $Cd(OH)_2 \rightarrow CdO + H_2O$. Of the two extremes at ~240 and ~300 °C for powders obtained from a zinc nitrate solution, only one is present in the spectrum of the mixture. These extremes correspond to the decomposition of zinc hyroxonitrates of various compositions to zinc oxide [9].

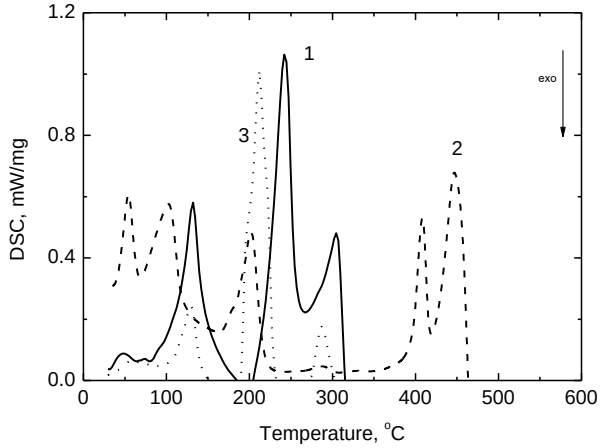

Fig. 6. DSC curves of calcination of powders obtaned from: 1- Zn nitrate [9], 2 – Cd nitrate [10], 3 – mixure of Zn and Cd nitrates
Рис. 6. Кривые ДСК прокаливания порошков, полученных из: 1 – нитрата Zn [9], 2 – нитрата Cd [10], 3 – смеси нитратов Zn и Cd

CONCLUSION

The action of the glow discharge onto the water solution of a mixture of zinc and cadmium nitrates lead to the formation of the powders in near-to-surface layer of the liquid anode. The powders formation kinetics in first approximation describes by the first order kinetics law. The synthesized powder exhibit crystallinity, has a complicated chemical composition and consists of hydroxides and hydroxynitrates of zinc and cadmium. When these powders are calcined, spherical granules with a size of 1-2 μm are formed. The granules are composed of zinc and cadmium oxides. Due to the different deposition rates of zinc and cadmium hydroxides, the granules are inhomogeneous. Cadmium compounds are predominantly located on the surface of the granules, while zinc compounds are located in the core. For the same reason, despite equal concentrations of zinc and cadmium ions in solution, the concentrations in the solid phase differ. The zinc content is greater than the cadmium content.

ACKNOWLEDGEMENTS

The study was carried out using the resources of the Center for Shared Use of Scientific Equipment of the ISUCT (with the support of the Ministry of Science and Higher Education of Russia, grant No. 075-15-2021-671).

This work was supported by the Ministry of High Education and Science of the Russian Federation, project No. FZZW-2020-0009 and by Russian Science Foundation № 22-22-00372 (rscf.ru/project/22-22-00372/).

The authors declare the absence a conflict of interest warranting disclosure in this article.

Исследование выполнено с использованием ресурсов Центра коллективного пользования научным оборудованием ИГХТУ (при поддержке Минобрнауки России, грант № 075-15-2021-671).

Работа выполнена при поддержке Министерства высшего образования и науки Российской Федерации, проект № FZZW -2020-0009 и Российского научного фонда № 22-22-00372 (rscf.ru/project/22-22-00372/).

Авторы заявляют об отсутствии конфликта интересов, требующего раскрытия в данной статье.

REFERENCES
ЛИТЕРАТУРА

1. **Huynh W.U., Dittmer J.J., Alivisatos A.P.** Hybrid Nanorod-Polymer Solar Cells. *Science*. 2002. V. 295. N 5564. P. 2425-2427. DOI: 10.1126/science.1069156.
2. **Bailey R.E, Smith A.M., Nie S.** Quantum dots in biology and medicine. *Physica E*. 2004. V. 25. N 1. P. 1-12. DOI: 10.1016/j.physe.2004.07.013.
3. **Ballou B., Lagerholm B.C., Ernst L.A., Bruchez M.P., Waggoner A.S.** Noninvasive Imaging of Quantum Dots in Mice. *Bioconjug. Chem.* 2004. V. 15. N 1. P. 79-86. DOI: 10.1021/bc034153y.
4. **Das D., Datta A.K., Kumbhakar D.V., Ghosh B., Pramanik A., Gupta S.** Conditional optimisation of wet chemical synthesis for pioneered ZnO nanostructures. *Nano-Struct. Nano-Objects*. 2017. V. 9. P. 26–30. DOI: 10.1016/j.nanoso.2016.12.002.
5. **Ghosh M., Raychaudhuri A.K.** Structure and optical properties of Cd-substituted ZnO ($Zn_{1-x}Cd_xO$) nanostructures synthesized by the high-pressure solution route. *Nanotechnology*. 2007. V. 18. N 11. P. 115618. DOI: 10.1088/0957-4484/18/11/115618.
6. **Raja S., Bhuvaneswari P.V., Ramesh Babu R., Gokulakrishnan V., Ramamurthi K.** Studies on the structural, morphological, electrical and optical properties of $(CdO)_x(ZnO)_{1-x}$ thin films deposited by spray pyrolysis method. *J. Mater. Sci: Mater. Electron.* 2016. V. 27. N 8. P. 8111–8117. DOI: 10.1007/s10854-016-4812-y.
7. **Sathish D.V., Rama Krishna Ch., Venkata Reddy Ch., Udayachandran Thampy U.S., Ravikumar R.V.S.S.N.** Structural and optical investigations on ZnCdO nanopowder. *Phys. Scr*. 2012. V. 86. N 3. P. 035708. DOI: 10.1088/0031-8949/86/03/035708.
8. **Detert D.M., Lim S.H.N., Tom K., Luce A.V., Anders A., Dubon O.D., Yu K.M., Walukiewicz W.** Crystal structure and properties of CdxZn1−xO alloys across the full composition range. *Appl. Phys. Lett*. 2013. V. 102. N 23. P. 232103. DOI: 10.1063/1.4884683.
9. **Shutov D.A., Rybkin V.V., Ivanov A.N., Smirnova K.V.** Synthesis of zinc oxide powders in plasma-solution systems. *High Energ. Chem.* 2017. V. 51. N 1. P. 65-69. DOI: 10.1134/S0018143917010118.

10. **Shutov D.A., Smirnova K.V., Gromov M.V., Ivanov A.N., Rybkin V.V.** Synthesis of CdO Ultradisperse Powders Using Atmospheric Pressure Glow Discharge in Contact With Solution and the Investigation of Intermediate Products. *Plasma. Chem. Plasma Process.* 2018. V. 38. N 1. P. 107-121. DOI: 10.1007/s11090-017-9856-0.
11. **Shutov D., Ivanov A., Rakovskaya A., Smirnova K., Manukyan A., Rybkin V.** Synthesis of oxygen-containing iron powders and water purification from iron ions by glow discharge of atmospheric pressure in contact with the solution. *J. Phys. D: Appl. Phys.* 2020. V. 53. N 44. P. 445202. DOI: 10.1088/1361-6463/aba4d7.
12. **Smirnova K.V., Shutov D.A., Ivanov A.N., Manukyan A.S., Rybkin V.V.** Plasma-Solution Synthesis of Iron (III) Oxide. *ChemChemTech [Izv. Vyssh. Uchebn. Zaved. Khim. Khim. Tekhnol.]*. 2021. V. 64. N 7. P. 83-88. DOI: 10.6060/ivkkt.20216407.6409. **Смирнова К.В., Шутов Д.А., Иванов А.Н., Манукян А.С., Рыбкин В.В.** Плазма-растворный синтез оксида железа (III). *Изв. вузов. Химия и хим. технология.* 2021. Т. 64. Вып. 7. С. 83-88. DOI: 10.6060/ivkkt.20216407.6409.
13. **Altomare A., Corriero N., Cuocci C., Falcicchio A., Moliterni A., Rizzi R.** QUALX2.0: a qualitative phase analysis software using the freely available database POW_COD. *J. Appl. Cryst.* 2015. V. 48. N 2. P. 598-603. DOI: 10.1107/S1600576715002319.
14. **Grazulis S., Daskevic A., Merkys A., Chateigner D., Lutterotti L., Quiros M., Serebryanaya N.R., Moeck P., Downs R.T., LeBail A.** Crystallography Open Database (COD): an open-access collection of crystal structures and platform for world-wide collaboration. *Nucl Acids Res.* 2012. V. 40. N D1. P. D420-427. DOI: 10.1093/nar/gkr900.
15. **Bobkova E.S., Shikova T.G., Grinevich V.I., Rybkin V.V.** Mechanism of Hydrogen Peroxide Formation in Electrolytic Cathode of Atmospheric_Pressure Direct_Current Discharge. *High Energ Chem.* 2012. V. 46. N 1. P. 56-59. DOI: 10.1134/S0018143912010079.
16. **He B., Ma Y., Gong X., Long Z., Li J., Xiong Q., Liu H., Chen Q., Zhang X., Yang S., Liu Q.H.** Simultaneous quantification of aqueous peroxide, nitrate, and nitrite during the plasma–liquid interactions by derivative absorption spectrophotometry. *J. Phys. D: Appl. Phys.* 2017. V. 50. N 44. P. 445207. DOI: 10.1088/1361-6463/aa8819.
17. **Lin J., He X., Chen Q., Xiong Q., Li J., Wang X., Chen G., Liu Q.H., Ostrikov K.** The formation mechanism of aqueous hydrogen peroxide in a plasma-liquid system with liquid as the anode. *Europ. Phys. J. D.* 2020. V. 74. N 4. Art. numb.: 80. DOI: 10.1140/epjd/e2020-100371-2.
18. **Shutov D.A., Batova N.A., Rybkin V.V.** Comparative Kinetics of Changing Chemical Composition of Liquid Water Anode and Cathode of DC Glow Discharge in Air. *High Energ. Chem.* 2020. V. 54. N 1. P. 59-63. DOI: 10.1134/S0018143920010117.
19. **Shutov D.A., Sungurova A.V., Choukourov A., Rybkin V.V.** Kinetics and mechanism of Cr(VI) Reduction in a Water Cathode Induced by Atmospheric Pressure DC Discharge in Air. *Plasma Chem. Plasma Process.* 2016. V. 36. N 5. P. 1253-1269. DOI: 10.1007/s11090-016-9725-2.
20. **Liu Z.C., Liu D.X., Luo S.T., Wang W.T., Liu Z.J., Yang A.J., Rong M.Z., Chen H.L., Kong M.G.** The effect of pH on the aqueous reactive species in sodium phosphate buffers induced by surface air discharge. *J. Phys. D: Appl. Phys.* 2019. V. 52. N 41. P. 415201. DOI: 10.1088/1361-6463/ab2f07.
21. **Zheng Y., Wang L., Bruggeman P.** Modeling of an atmospheric pressure plasma-liquid anodic interface: Solvated electrons and silver reduction. *J. Vac. Sci. Technol.* 2020. V. A38. N 6. P. 063005. DOI: 10.1116/6.0000575.
22. **Buxton G.V., Greenstock C.L., Helman W.P., Ross A.B.J.** Critical review of rate constants for reactions of hydrated electrons, hydrogen atoms and hydroxyl radicals (OH/O^-) in aqueous solution. *Phys. Chem. Ref. Data.* 1988. V. 17. N 2. P. 513–886. DOI: 10.1063/1.555805.
23. **Rumbach P., Bartels D.M., Sankaran R.M., Go D.B.** The solvation of electrons by an atmospheric-pressure plasma. *Nat. Comm.* 2015. V. 6. P. 7248. DOI: 10.1038/ncomms8248DOI:38/ncomms8248.
24. **Ivanov A.N., Shutov D.A., Manukyan A.S., Rybkin V.V.** Influence of Non-uniformity of Generation of Active Particles on Deposition Processes and Redox Reactions in a Glow Discharge in Contact with Water. *Plasma Chem. Plasma Process*. 2019. V. 39. N 1. P. 63-73. DOI: 10.1007/s11090-018-9936-9.
25. **Witzke M., Rumbach P., Go D.B., Sankaran R.M.** Evidence for the electrolysis of water by atmospheric-pressure plasmas formed at the surface of aqueous solutions. *J. Phys. D: Appl. Phys.* 2012. V. 45. N 7. P. 442001. DOI: 10.1088/0022-3727/45/44/442001.
26. **Rumbach P., Bartels D.M., Go D.B.** The penetration and concentration of solvated electrons and hydroxyl radicals at a plasma-liquid interface. *Plasma Sours. Sci. Technol.* 2018. V. 27. N 11. P. 115013. DOI: 10.1088/1361-6595/aaed07.
27. **Mededovic Thagard S., Takashima K., Mizuno A.** Chemistry of the Positive and Negative Electrical Discharges Formed in Liquid Water and Above a Gas–Liquid Surface. *Plasma Chem. Plasma Process.* 2009. V. 29. N 6. P. 455-473. DOI: 10.1007/s11090-009-9195-x.

Поступила в редакцию 25.01.2022
Принята к опубликованию 21.04.2022

Received 25.01.2022
Accepted 21.04.2022